(Received 11 December 2023, Accepted 2 January 2024, Scheduled 18 January 2024)

Dual-Feed Orthogonally Polarized Compact 8-Element MIMO Antenna Using Metallic Stub and Decoupling Unit for Isolation Enhancement of Sub-6 GHz 5G Application

Munusami Cholavendan and Venkatesan Rajeshkumar*

Department of Communication Engineering, School of Electronics Engineering
Vellore Institute of Technology, Vellore, Tamilnadu, India

ABSTRACT: A compact dual-feed multiple-input multiple-output (MIMO) antenna is designed for sub-6 GHz 5G applications with isolation enhancement. The proposed dual-polarized MIMO antenna formed by each patch uses two inset-feed lines placed orthogonal to each other with symmetric conditions, which excite each port to resonate at the same frequency (3.65 GHz). The stub is identified diagonally based on plated through-hole technology between orthogonal ports. The structure employs a half mode and maintains minimum inter-port isolation (≤ -12 dB) of each patch, followed by another patch to form an 8-element miniaturized MIMO antenna. High isolation (≤ -15 dB) is achieved with the help of a decoupling structure placed between the antennas in the ground plane. Measurements of a fabricated prototype validate the simulation results. The diversity performances of MIMO antenna parameters like envelope correlation coefficient (ECC), diversity gain (DG), and Mean Effective Gain (MEG) are also found within acceptable ranges.

1. INTRODUCTION

With the progress of wireless communications technology, multiple-input multiple-output (MIMO) technology can enhance high data rates for its channel capacity and required consistent signal quality in 5G communication [1]. However, it is very challenging to integrate more antenna elements due to the constrained spaces suggested by handheld devices. When antenna units are placed close together, isolations will substantially deteriorate [2]. It becomes a significant challenge for antenna engineers to figure out more antenna for handheld devices with less space and high isolation.

As the literature mentions, some techniques have been attempted to shrink the antenna space and improve isolation. To get one or more than one band, dual-feed/dual-polarization, di/tri/quad-flexing, and slot/stub techniques are used to minimize the antenna footprint. In this way, the dual-feed/polarization can be an excellent alternative to conventional miniaturized single-band operation [3, 4]. Moreover, the antenna footprint with sustained port isolation explores new ideas based on SIW self-multiplexing antenna [5–7]. In MIMO, orthogonally polarized elements are highly isolated from each other [8–11]. Further, by utilizing various decoupling structures, it is possible to improve the isolation between elements [1, 12–21].

Dual-feed antenna is used in modern MIMO communication systems to reduce antenna footprint. More than one port in a single radiator [22] or dual polarized radiators have orthogonal feeds typically found in handheld electronics [23–25]. The dual-feed MIMO structure was reported to minimize the size of the elements as well as the coupling factor between the ports presented for single/multi-band/wideband antenna [26–29].

In this paper, a compact dual-feed dual-polarized 8-element MIMO antenna is presented. The proposed MIMO antenna offers a compact shape. Each square patch comprises two dual feeds that are orthogonally positioned and operating at 3.65 GHz with dual polarization. Instead of using a cavity-backed substrate integrated waveguide (SIW), a novel metallic stub is loaded diagonally between two ports to obtain inter-port isolation of less than -22 dB with excited half mode TE_{110} at each port. A plus-shaped slotted-decoupling structure is added to the back of the ground plane to achieve a high isolation of -58.46 dB. The performance of the 8-element MIMO antenna was evaluated using simulated and measured characteristics. Moreover, the designed antenna's surface current distribution and diversity metrics are examined. A compact 8-element MIMO antenna has been developed for Wi-Max, radio altimeter, 5G wireless receiver front end, and S-band applications.

2. ANTENNA CONFIGURATION

The structural design of the proposed 8-element MIMO antenna ($48 \times 48 \times 1.6\,\text{mm}^3$) is depicted in Fig. 1. The MIMO structure is made up of four individual patches. Each patch has two inset feed 50 Ω lines arranged in an orthogonal, symmetrical relationship to excite the resonance at the same frequency. The 8-element MIMO antenna is comprehended on a single-layer FR-4 substrate having dielectric permittivity ($\epsilon_r = 4.4$), loss tangent ($\tan\delta = 0.02$), and thickness 1.6 mm, which is an inexpensive substrate. The performance results are examined by an electromagnetic simulator using the CST studio suite.

* Corresponding author: Venkatesan Rajeshkumar (vrajeshme@gmail.com).

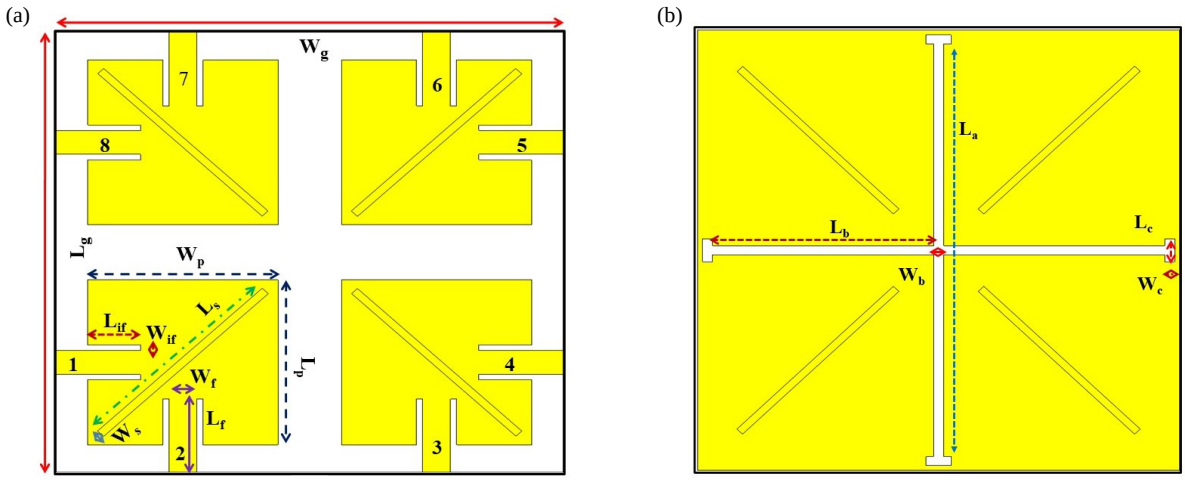

FIGURE 1. Geometry of the proposed 8-element MIMO antenna. (a) Top layer. (b) Bottom layer. ($W_g = 48$, $L_g = 48$, $W_p = 18$, $L_p = 18$, $W_f = 2.6$, $L_f = 8$, $W_{if} = 0.6$, $L_{if} = 5$, $W_s = 0.8$, $L_s = 22$, $L_a = 47$, $W_b = 1$, $L_b = 22$, $W_c = 1$, $L_c = 2.5$; Units: mm).

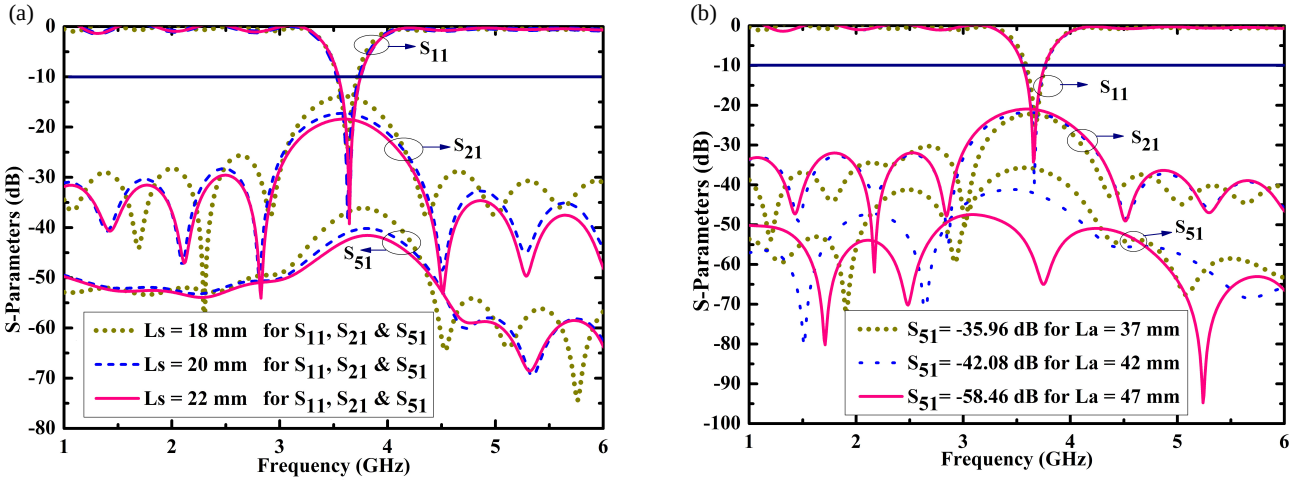

FIGURE 2. Parametric characteristics of 8-element MIMO simulated S-parameters, optimized value of (a) metallic stub (Ls) added without any decoupling unit, (b) decoupling structure (La) at 3.65 GHz.

3. EIGHT ELEMENT MIMO ANTENNA ANALYSIS

An essential four-unit block makes the dual-polarized 8-element MIMO antenna. Each unit is designed by using a dual 50 Ω inset feed line with a metallic stub. In most of the literature, half mode (HM) or quatre mode (QM) was obtained from cavity-backed SIW antenna for size reduction. The novelty of this work is each patch has two orthogonal feed excitations; a metallic stub placed diagonally is loaded from top to bottom through the substrate between two ports, as a method followed by copper-filled within the stub through the surface. Its radiating half mode, as well as both polarizations (vertical and horizontal polarizations), operates at the same frequency of 3.65 GHz and maintains inter-port isolation of less than −12 dB. Moreover, patches are arranged orthogonally with sufficient isolation better than −15 dB for the four antenna units. A plus-shaped slot decoupling structure (S-DCS) was placed among the patches in the ground plane to improve isolation further.

3.1. Parametric Analysis of Miniaturized MIMO Antenna

The parametric analysis is performed on the proposed 8-element MIMO antenna for optimized performance. To understand the S_{11} characteristics, a parametric study was performed on specific parameters, such as the length of the metallic stub placed diagonally between two ports and the plus-shaped decoupling structure.

First, optimetrics was accomplished by adjusting the length of metallic stub Ls from 18 to 22 mm while maintaining another parameter constant. Meanwhile, to see the effect of S-parameters such as reflection coefficient (return loss), the transmission coefficients are self-isolation (S_{21}) and isolation (S_{51}) at the operating frequency of 3.65 GHz, as shown in Fig. 2.

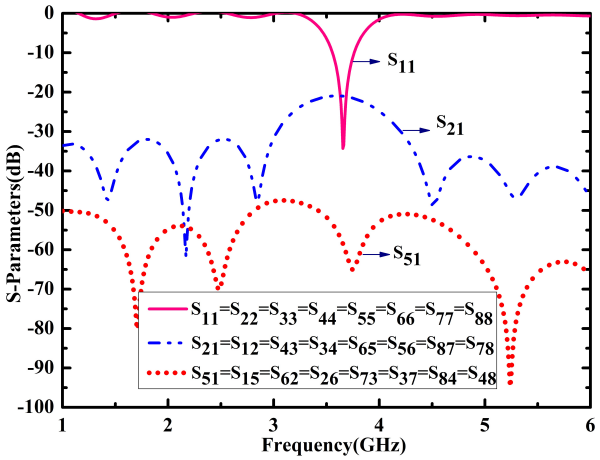

FIGURE 3. Simulated S-parameters characteristics of 8-element MIMO antenna.

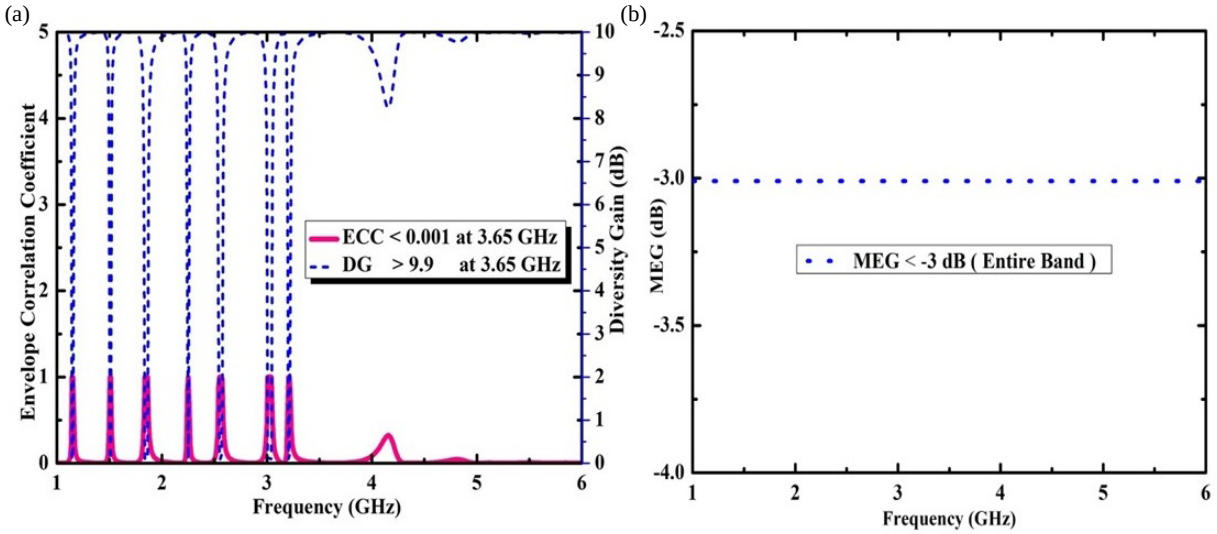

FIGURE 4. MIMO metrics, (a) ECC & DG, (b) MEG.

The influence of metallic stub length on S-parameters characteristics was studied. As the parameter Ls grows without any modification on operating band frequency (3.65 GHz), transmission coefficient ($S_{21} = -18$ dB and $S_{51} = -42$ dB) achieves a better response without any decoupling structure of optimized value stub length ($Ls = 22$ mm), as shown in Fig. 2(a).

Similarly, the optimetrics were performed on a plus-shaped decoupling structure to improve isolation performance. The rectangular plus shape slotted-decoupling structure (S-DCS) was introduced in the ground plane. The variable length (La) of S-DCS varied from 37 to 47 mm, as shown in Fig. 2(b). It has been observed that maximum isolation ($S_{51} = -58.46$ dB) and inter-port isolation ($S_{21} = -22$ dB) are achieved at 3.65 GHz for the optimized S-DCS parameter ($La = 47$ mm). The isolation of 16.46 dB is improved using a plus-shape slotted-decoupling structure (S-DCS) compared with that without any extra unit added between the elements. Hence, the 8-element dual-feed MIMO antenna achieved maximum isolation using S-DCS.

3.2. Analysis of S-Parameters, MIMO Parameters and Surface Current Distribution

3.2.1. Investigation of MIMO S-Parameters

The proposed 8-element MIMO antenna, simulated S-parameters results, performance metrics, and surface current flow are shown in Figs. 3, 4, and 5. Four pairs of dual-feed square patches are orthogonally placed with uniform structures and dimensions. Consequently, the dual-polarized antenna is attempted to present in a novel MIMO structure for miniaturization and high isolation purposes.

The S-parameter characteristics of each port are depicted in Fig. 3. From the results, the antenna covers the entire bandwidth of 210 MHz (3.557 to 3.767 GHz) at 3.65 GHz with a reflection coefficient of less than -35 dB for a dual-polarized MIMO antenna. The inter-port isolation between port-1 and port-2 of -22 dB is achieved, and high isolation is obtained between port-1 and port-5 of -58.46 dB using a plus-shaped slot decoupling structure placed in the ground plane. Similarly,

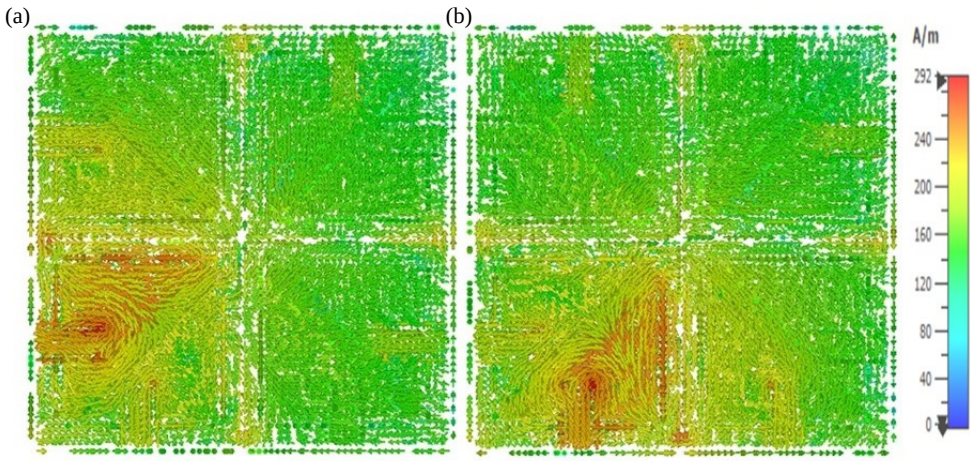

FIGURE 5. Surface current distribution, (a) port-1, (b) port-2.

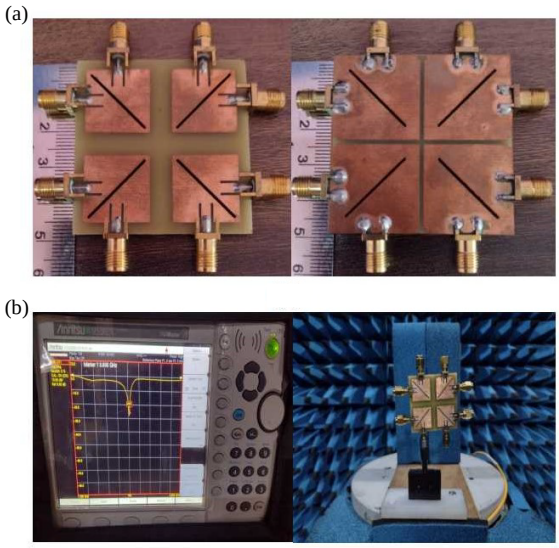

FIGURE 6. 8-element MIMO, (a) fabricated antenna, (b) measurement setup.

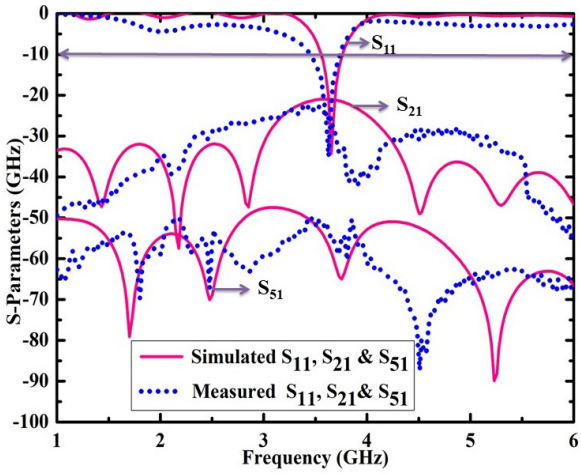

FIGURE 7. Simulated and measured S-parameters characteristics of MIMO antenna.

other port results are shown in Fig. 3. Hence, all the ports' S-parameter results are almost the same at 3.65 GHz.

3.2.2. MIMO Parameters

The MIMO antenna parameters, such as Envelope Correlation Coefficient (ECC), Diversity Gain (DG), and Mean Effective Gain (MEG), are investigated. ECC and DG values are evaluated from far-field equations (1) and (2) for better accuracy [21], and MEG is also a very important parameter; at each port, it can be evaluated from the S-parameter equation (3) as follows [30].

$$\mathrm{ECC}(\rho_{ij}) = \frac{\iint_{4\pi} \left|\overline{F_i}(\theta,\phi)\cdot\overline{F_j}(\theta,\phi)d\Omega\right|^2}{\iint_{4\pi}\left|\overline{F_i}(\theta,\phi)\right|^2 d\Omega \iint_{4\pi}\left|\overline{F_j}(\theta,\phi)\right|^2 d\Omega} \quad (1)$$

$$\mathrm{DG} = 10\sqrt{(1-\mathrm{ECC})^2} \quad (2)$$

$$\mathrm{MEG}(i) = 0.5\left[1 - \sum_{j=1}^{N}|Sij|^2\right] \quad (3)$$

In the MIMO system, the correlation among ports, the value of ECC should be lower than 0.0001 with DG as a value greater than 9.99 dB, as depicted in Fig. 4(a). Additionally, MEG has less than -3 dB in each port's working band, as shown in Fig. 4(b). It means that the MIMO antenna achieved better diversity performance. Hence, the proposed antenna is more suitable for MIMO applications.

3.2.3. Surface Current Distribution of 8-Element MIMO

The MIMO antenna's E-field distribution with corresponding port excitation is depicted in Fig. 5. The whole mode is divided into two equal parts, and each piece is called half mode. It is due to stubs being placed diagonally based on plated through-hole technology between orthogonal ports. It indicates that the

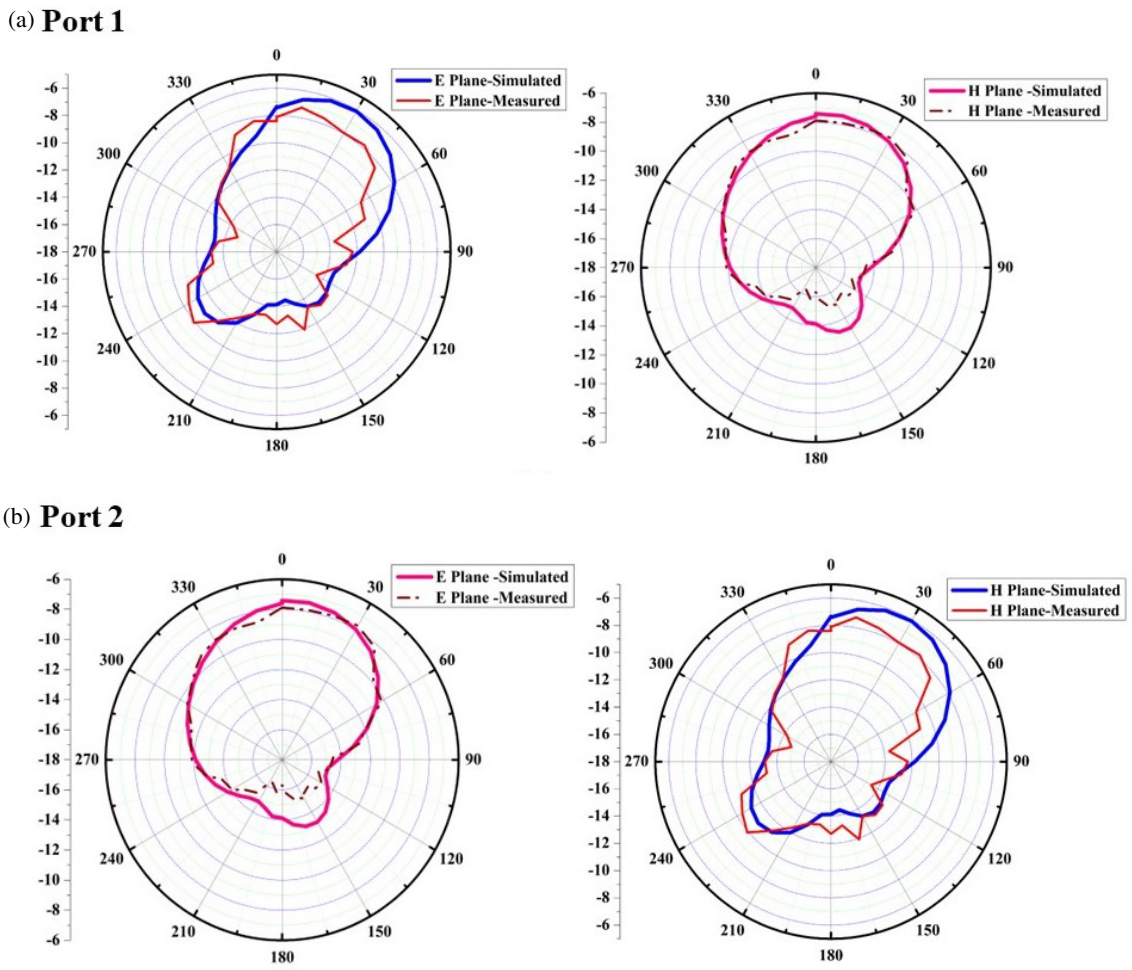

FIGURE 8. The simulated and measured radiation performance of E and H plane, (a) port-1, (b) port-2.

fundamental mode TE_{110} is excited at each port, resonating at 3.65 GHz; when port-1 is excited, the other ports are matched with the termination of 50 Ω. Due to the excitation of each port, the maximum electric field intensity dominates the corresponding port excitation and transmits a minimal amount of field to other ports. This is clearly shown in the surface current distribution of respective port-1, port-2, etc.

Each patch has two ports that can be excited independently to produce two orthogonally polarized waves. Specifically, when port-1 is excited, the horizontaly polarised wave is radiated in one of the directions, as shown in Fig. 5(a). At the same time, another direction, a vertically polarized wave, is generated when port-2 is excited, as shown in Fig. 5(b). The remaining elements are orthogonally placed concerning each other. Hence, out of 8 elements, four horizontally polarized and four vertically polarized are formed in the MIMO structure.

4. EXPERIMENTAL VALIDATION

Photographs of the fabricated and measured setup for the proposed 8-element MIMO antenna are shown in Fig. 6. The far-field measurement results obtained using an Anritsu VNA (MS20227C) with an anechoic chamber for the proposed 8-element MIMO antenna are shown in Figs. 6(a) and 6(b).

The comparison between simulated and measured S-parameters with radiation pattern results is represented in Fig. 7 and Fig. 8. The MIMO antenna operates at a frequency of 3.65 GHz when port-1 is excited, and the remaining ports are terminated. In all cases, the reflection coefficient (S_{11}) is -34 dB; inter-port isolation (S_{21}) is less than -22 dB; and high isolation (S_{51}) is less than -58 dB which has been measured among the ports, as shown in Fig. 7. Similarly, measure S-parameters when other ports are excited.

When port-1 is excited, the normalized far-field radiation patterns in H-plane ($\phi = 90°$) and E-plane ($\phi = 0°$) are measured at 3.65 GHz, and the remaining ports are matched with the termination of 50 Ω loads. Then, when port-2 is exited, the other ports are terminated, and corresponding E and H far-field radiation patterns are measured at 3.65 GHz, as shown in Fig. 8.

Finally, comparing the port-1 and port-2 results, the radiation patterns E and H are interchanged because ports are positioned orthogonally. Due to orthogonal placement, port-1 produces horizontal polarization, and port-2 creates vertical polarization. Similarly, measure the radiation pattern for the remaining ports. Hence, the E and H radiation patterns are interchanged or mir-

TABLE 1. Comparison of the proposed antenna with in literature.

Ref.#	Size (mm^3)	Frequency /(GHz)	Patch/Feed per Patch	Total Elements	Dual Polarization	Isolation/Method	ECC	DG
[1]	$47.5 \times 45 \times 1.6$	3.5	2/1	2	NO	-20 dB/MTM-SRR	< 0.05	-
[12]	$50 \times 50 \times 1.6$	4.3–6.45	4/1	4	NO	-20 dB/Orthogonal	< 0.004	> 9.99
[13]	$60 \times 60 \times 1.6$	1.89	4/1	4	NO	-20 dB/Orthogonal + SIW	< 0.03	-
[14]	$130 \times 98 \times 1.6$	2.5	2/1	2	NO	-36 dB/L-shape Stub + DGS	< 0.002	> 9.9
[15]	$50 \times 30 \times 1.6$	3.5	2/1	2	NO	-28 dB/DGS	< 0.0004	> 9.99
[16]	$95.94 \times 38.20 \times 1.6$	2.47	2/1	2	NO	-24.67 dB/EBG	< 0.008	-
[17]	$48 \times 48 \times 1.6$	3.5	4/1	4	NO	-38 dB/Orthogonal + EBG	< 0.0002	> 9.99
[18]	$140 \times 45 \times 1.6$	4.9	4/1	4	NO	-25 dB/DRA placing 180° phase	< 0.002	> 9.99
[19]	$120 \times 73 \times 0.8$	5.65	4/2	8	NO	-25.4 dB/DNG Metasurface	< 0.003	> 9.98
[21]	$60 \times 60 \times 1.6$	3.26–5.18	4/1	4	NO	-15 dB/Orthogonal + Stub	< 0.005	~ 10
[22]	$150 \times 80 \times 0.8$	3.5	6/1	6	NO	-18 dB/L-shaped Monopole + Slots	< 0.03	-
[23]	$75 \times 150 \times 1.6$	3.6 GHz	4/2	8	Yes	-17 dB/Orthogonal	< 0.03	-
[26]	$330 \times 330 \times 0.8$	1.35 GHz/ 1.76 GHz	4/2	8	Yes	-20.2 dB/Orthogonal + Metal Strips DCS	-	-
[27]	$75 \times 150 \times 1.6$	3.6 GHz	4/2	8	Yes	-20 dB/Orthogonal + CSSR loaded	< 0.04	-
[28]	$70 \times 70 \times 1.6$	3.15–6 GHz	4/2	8	Yes	-36 dB/Orthogonal + Circular Parasitic Unit	< 0.0001	> 9.99
[29]	$70 \times 70 \times 1.6$	3.5–6 GHz	4/2	8	Yes	-24 dB/Orthogonal + Vias array metallic strip	< 0.05	> 9.9
This work	$48 \times 48 \times 1.6$	3.65 GHz	4/2	8	Yes	-58.46 dB/Orthogonal + S-DCS	< 0.0001	> 9.99

ror images depending on the position and distances. However, due to fabrication tolerance, the simulation environment's limitations, or soldering imperfections, measured results slightly differ from those predicted by simulation results.

The proposed 8-element MIMO antenna is compared within the literature in Table 1. The antenna elements are placed orthogonally to each other to achieve better isolation. In addition, various decoupling structures are discussed in the survey, such as DGS, Parasitic Unit, EBG, Metamerial, and Metasurface, and Vias Array Metallic Strips are placed between antennas to enhance the isolation further. MIMO structures discussed so far make a complex design, huge size, and sufficient isolation. The proposed MIMO antenna used dual-feed orthogonally polarized with a metallic stub and plus-shaped slot decoupling unit for isolation enhancement. This design has advantages such as a small antenna footprint, simple design, high isolation, low correlation between nearby antennas, and low-cost fabrication. Consequently, it is appropriate for 5G MIMO applications.

5. CONCLUSION

A novel dual-fed MIMO antenna with enhanced isolation is investigated. A radiating 2×4 element MIMO antenna comprises four patches with dual feeds arranged in an orthogonal position and operated at 3.65 GHz. Due to orthogonal feed lines and stub loading, which results in compact (size miniaturization) and inter-port isolation more significant than -22 dB, as well as fundamental mode, TE_{110} is excited. The proposed 8-element MIMO antenna exhibits high isolation (< -58 dB) obtained by a plus-shaped decoupling structure employed in the ground plane between the antennad. Due to the low correlation among the elements, the antenna has typical ECC (< 0.0001), high DG (> 9.99 dB), and MEG (< -3 dB), which is close to the ideal value, hence most suitable for Wi-Max, radio altimeter, 5G wireless receiver front end, S-band, and sub-6 GHz 5G MIMO application.

REFERENCES

[1] Wang, C., X.-S. Yang, and B.-Z. Wang, "A metamaterial-based compact broadband planar monopole MIMO antenna with high isolation," *Microwave and Optical Technology Letters*, Vol. 62, No. 9, 2965–2970, 2020.

[2] Babu, K. V. and B. Anuradha, "Design of MIMO antenna to interference inherent for ultra wide band systems using defected ground structure," *Microwave and Optical Technology Letters*, Vol. 61, No. 12, 2698–2708, 2019.

[3] Dash, S. K. K., Q. S. Cheng, R. K. Barik, T. Khan, and K. S. Subramanian, "A compact dual-fed highly isolated SIW based self-diplexing antenna," *AEU-International Journal of Electronics and Communications*, Vol. 132, 153613, 2021.

[4] Barik, R. K., S. Koziel, Q. S. Cheng, and S. Szczepanski, "Highly miniaturized self-diplexed U-shaped slot antenna based on shielded QMSIW," *IEEE Access*, Vol. 9, 158 926–158 935, 2021.

[5] Dash, S. K. K., Q. S. Cheng, R. K. Barik, N. C. Pradhan, and K. S. Subramanian, "A compact triple-fed high-isolation SIW-based self-triplexing antenna," *IEEE Antennas and Wireless Propagation Letters*, Vol. 19, No. 5, 766–770, 2020.

[6] Kumar, A. and S. Raghavan, "Design of SIW cavity-backed self-triplexing antenna," *Electronics Letters*, Vol. 54, No. 10, 611–612, 2018.

[7] Dash, S. K. K., Q. S. Cheng, and R. K. Barik, "A compact substrate integrated waveguide backed self-quadruplexing antenna for c-band communication," *International Journal of RF and Microwave Computer-Aided Engineering*, Vol. 30, No. 10, 1–9, 2020.

[8] Keshri, P. K., R. Chandel, S. K. Sahu, and A. K. Gautam, "Compact quad-port high performance UWB MIMO/diversity antenna with slotted ground structure," *Progress In Electromagnetics Research C*, Vol. 112, 193–205, 2021.

[9] Naktong, W. and A. Ruengwaree, "Four-port rectangular monopole antenna for UWB-MIMO applications," *Progress In Electromagnetics Research B*, Vol. 87, 19–38, 2020.

[10] Achariparambil, A., P. Thomas, K. K. Indhu, K. Neema, R. A. Kumar, and A. Chandroth, "Four-element compact and dual-band MIMO antenna with self-decoupled mechanism for 5G applications," *Progress In Electromagnetics Research C*, Vol. 123, 91–99, 2022.

[11] Mathur, R. and S. Dwari, "Compact 4-port MIMO/diversity antenna with low correlation for UWB application," *Frequenz*, Vol. 72, No. 9-10, 429–435, 2018.

[12] Mohammad Saadh, A. W., S. Khangarot, B. V. Sravan, N. Aluru, P. Ramaswamy, T. Ali, and M. M. M. Pai, "A compact four-element MIMO antenna for WLAN/WiMAX/satellite applications," *International Journal of Communication Systems*, Vol. 33, No. 14, 1–17, 2020.

[13] Sung, Y., "Closely spaced MIMO antenna based on substrate-integrated waveguide technology," *Microwave and Optical Technology Letters*, Vol. 60, No. 7, 1794–1798, 2018.

[14] Li, Y., L.-A. Bian, K.-D. Xu, Y. Liu, Y. Wang, R. Chen, and S. Xie, "Mutual coupling reduction for monopole MIMO antenna using L-shaped stubs, defective ground and chip resistors," *AEU - International Journal of Electronics and Communications*, Vol. 160, 154524, 2023.

[15] Babu, K. V., S. Das, G. N. J. Sree, S. K. Patel, M. P. Saradhi, and M. R. N. Tagore, "Design and development of miniaturized MIMO antenna using parasitic elements and machine learning (ML) technique for lower sub 6 GHz 5G applications," *AEU - International Journal of Electronics and Communications*, Vol. 153, 154281, 2022.

[16] Sharma, K. and G. P. Pandey, "Two port compact MIMO antenna for ISM band applications," *Progress In Electromagnetics Research C*, Vol. 100, 173–185, 2020.

[17] Tamminaina, G. and R. Manikonda, "Investigation on performance of four port MIMO antenna using electromagnetic band gap for 5G communication," *Progress In Electromagnetics Research M*, Vol. 119, 51–62, 2023.

[18] Sarkar, G. A., S. Ballav, A. Chatterjee, S. Ranjit, and S. K. Parui, "Four element MIMO DRA with high isolation for WLAN applications," *Progress In Electromagnetics Research Letters*, Vol. 84, 99–106, 2019.

[19] Sharma, R., R. Khanna, and G. Singla, "A miniaturized highly isolated double negative metasurface MIMO antenna for sub-6 GHz band," *Sadhana - Academy Proceedings in Engineering Sciences*, Vol. 47, No. 4, 202, 2022.

[20] Zou, X., G. M. Wang, Y. W. Wang, and B. F. Zong, "Decoupling of dual-band closely spaced MIMO antennas based on novel coupled resonator structure," *Frequenz*, Vol. 72, No. 9-10, 437–441, 2018.

[21] Addepalli, T., T. Vidyavathi, K. Neelima, M. Sharma, and D. Kumar, "Asymmetrical fed Calendula flower-shaped four-port 5G-NR band (n77, n78, and n79) MIMO antenna with high diversity performance," *International Journal of Microwave and Wireless Technologies*, Vol. 15, No. 4, 683–697, 2023.

[22] Rajesh, K. D. and B. G. Venkat, "Efficient and optimized six-port MIMO antenna system for 5G smartphones," *Frequenz*, Vol. 75, No. 11-12, 501–512, 2021.

[23] Parchin, N. O., A. S. I. Amar, M. Darwish, K. H. Moussa, C. H. See, R. A. Abd-Alhameed, N. M. Alwadai, and H. G. Mohamed, "Four-element/eight-port MIMO antenna system with diversity and desirable radiation for sub 6 GHz modern 5G smartphones," *IEEE Access*, Vol. 10, 133 037–133 051, 2022.

[24] Parchin, N. O., H. J. Basherlou, Y. I. A. Al-Yasir, A. M. Abdulkhaleq, R. A. Abd-Alhameed, and P. S. Excell, "Eight-port MIMO antenna system for 2.6 GHz LTE cellular communications," *Progress In Electromagnetics Research C*, Vol. 99, 49–59, 2020.

[25] Kumar, A., S. K. Mahto, R. Sinha, and A. Choubey, "Dual circular slot ring triple-band MIMO antenna for 5G applications," *Frequenz*, Vol. 75, No. 3-4, 91–100, 2021.

[26] Liu, J., H. Liu, X. Dou, Y. Tang, C. Zhang, L. Wang, R. Tang, and Y. Yin, "A low profile, dual-band, dual-polarized patch antenna with antenna-filter functions and its application in MIMO systems," *IEEE Access*, Vol. 9, 101 164–101 171, 2021.

[27] Kaushal, V., A. Birwal, and K. Patel, "Diversity characteristics of four-element ring slot-based MIMO antenna for sub-6-GHz applications," *ETRI Journal*, Vol. 45, No. 4, 581–593, 2023.

[28] Naser, H. M., O. A. Al-Ani, and M. F. Mosleh, "W-shaped eight-port wideband MIMO antenna," *Progress In Electromagnetics Research C*, Vol. 134, 211–222, 2023.

[29] Kaur, I., B. Basu, and A. Singh, "Sub-6 GHz metallic via integrated MIMO antenna array for 5G smartphone," *Progress In Electromagnetics Research C*, Vol. 138, 91–104, 2023.

[30] Addepalli, T., J. C. Rao, P. R. Sura, B. V. Ramana, and V. Satyanarayana, "Compact 'Q'-shaped connected ground 4-element MIMO antenna for X-band applications," *Progress In Electromagnetics Research C*, Vol. 130, 117–126, 2023.